JOURNAL OF CHEMICAL ENGINEERING AND INDUSTRIAL BIOTECHNOLOGY
E-ISSN: 0126-8139
VOLUME 11, ISSUE 2, OCTOBER 2025, 11 – 21
DOI: https://doi.org/10.15282/jceib.v11i2.12475

RESEARCH ARTICLE

Magnetic CNT Microfibrillated Cellulose of Sugarcane Bagasse (mCNT-MFCSCB) Foam as Oil Sorbent

Syazana Ab Manaf[1], Norsyamira Liyana Sulaiman[1], Yusilawati Ahmad Nor[1]*, Dzun Noraini Jimat[1], Kim Yeow Tshai[2]

[1] Department of Chemical Engineering and Sustainability, Kulliyyah of Engineering, International Islamic University Malaysia (IIUM), Jalan Gombak, 53100 Kuala Lumpur, Malaysia

[2] Department of Mechanical, Materials and Manufacturing Engineering, Faculty of Science and Engineering, University of Nottingham Malaysia, Jalan Broga, 43500 Semenyih, Selangor, Malaysia

ABSTRACT - Adsorption/absorption methods are among the popular approaches to clean oil contaminants on water surfaces due to their simplicity, efficiency, and low cost. To date, there is still ongoing research to develop oil sorbent material with high oil selectivity and, thus, high sorption capacity using environmentally friendly approaches. Herein, we proposed the development of a new oil sorbent in the form of porous carbon foam prepared from plant-based microcellulose fiber that is eco-friendly, non-toxic, reasonably cheap, and efficient, thereby promising a potential industry-adaptable approach. Three-dimensional (3D) crosslinked microfibrillated cellulose of sugarcane bagasse (MFCSCB) foams were first prepared as a base material, and magnetic ferrite nanoparticles (Fe_3O_4) and carbon nanotubes (CNTs) were further mixed into the structure of MFCSCB foam to impose hydrophobic property and introduce magnetic behaviour required as a good oil sorbent material. The foam comprises a 3D interconnected structure of cellulose microfiber with high porosity embedded with CNT/Fe_3O_4 nanocomposite. Maximum oil sorption efficiency is achieved using Design Expert Software, where the response surface method (RSM) with a three-level, three-factor full factorial design was used. Independent factors selected in the preparation of the mCNT-MFC composite foams were the percentage of CNTs, freezing temperature, and sonication time. The sample with the highest oil sorption performance (5.05 ± 0.5 g/g) was obtained at 0.75% CNT, -140 °C freezing time, and a sonication time of 20 minutes. Data inserted for the oil sorption optimization was the average value of triplicate samples with an average standard deviation of 0.5. The optimum sample was further characterized in detail using FESEM, FTIR, and XRD to understand the mechanism of oil sorption. The recyclability potential and oil sorption kinetics of the sample were also investigated. The mCNT-MFCs can selectively remove the oil from the oil/water interface with good oil sorption efficiency due to the presence of a highly porous structure and hydrophobic properties possessed by the composite, as well as easy oil recovery by a solvent removal approach.

ARTICLE HISTORY
Received : 20th May 2025
Revised : 1st Sep. 2025
Accepted : 2nd Sep. 2025
Published : 30th Dec. 2025

KEYWORDS
Oil sorbent
Sugarcane bagasse
Microfibrillated cellulose
Carbon nanotubes
Porous carbon foam
Oil-spill remediation

1.0 INTRODUCTION

Oil spills on rivers and seas have huge and immediate adverse economic, social, and environmental impacts. Several available methods to remediate oil spills, such as in-situ burning, dispersant and boom, and skimmers, do not provide a favourable solution in terms of cost, ease of deployment, significant resources, and environmentally friendly approach [1-3]. Since oil spills have occurred ever since the use of fossil fuels in society, there is an alarm requiring alternative strategies to tackle the limitations of the currently available methods. Several alternative solutions were proposed to satisfy some of these requirements, including adsorption methods using adsorbents of different compositions, such as polyurethane sponge, polyvinyl alcohol (PVA) aerogel, graphene sponges, and ion exchange resin [4]. Adsorption and absorption through oil-sorbent materials are commonly regarded as the preferred technological solution due to their comparatively affordable cost and high effectiveness [5]. However, oil sorbents are mostly prepared using non-green materials, which are made from non-degradable polymers, which can further expose substantive waste to the environment. Moreover, some of them are either extremely expensive or require expensive precursors [6].

In recent years, a great effort has been made to develop three-dimensional (3D) oil sorbent material using biodegradable, renewable, eco-friendly, and non-toxic organic compounds such as cellulosic materials from biomass [6]. Hydrogels made of micro-cellulose and nano-cellulose fibre extracted from agricultural waste such as palm oil husk or sugarcane bagasse are among the popular choices [7][8]. However, they suffered from low oil sorption capacity due to the hydrophilic nature of the celluloses, which are rich with the hydroxyl functional group, while oil is known for its

*CORRESPONDING AUTHOR | Yusilawati Ahmad Nor | ✉ yusilawati_ahmadnor@iium.edu.my

hydrophobic and oleophilic behaviour due to the presence of hydrocarbon compositions. Following this, a few studies have chemically modified the cellulose with silane functional groups such as methyltrimethoxysilane (MTMS) [8] and hexadecyltrimethoxysilane (HDTMS) [9] to increase hydrophobicity. However, this approach involves complicated steps, inconsistent product quality, altered biodegradability, and can be toxic to the environment [7]. Furthermore, cellulosic material cannot be recycled due to its higher swelling behaviour [16]. In a few other studies, the 3D cellulose hydrogels/foam were converted to carbon composition through pyrolysis to reduce their hydrophilicity and increase chemical stability [4][10]. Although this strategy enabled high oil sorption capacity (up to 87 g/g) and recyclability, the natural behaviour of the cellulose, such as degradability, was sacrificed. Thus, developing oil sorbent material from cellulosic-based material with an environmentally friendly approach is still challenging.

Herein, we proposed the development of a 3D magnetic CNT microfibrillated cellulose (mCNT-MFC) composite foam as an oil sorbent material using the freeze-drying method. As depicted in Figure 1, micro-fibrillated cellulose was first extracted from sugarcane bagasse using the alkaline bleaching method. The crosslinked micro-fibrillated cellulose foams were further incorporated with carbon nanotubes (CNT) and magnetic ferrite (MFe_2O_4) nanoparticles to produce mCNT-MFC with hydrophobic/oleophilic and magnetic properties. CNTs were added into the 3D framework of the micro-fibrillated cellulose due to their excellent potential for oil-water separation with low density, hydrophobic, and oleophilic nature, as well as large specific surface area. Meanwhile, MFe_2O_4 nanoparticles have been incorporated into the MFC framework to enable easy sample recovery. The mCNT-MFC was able to selectively remove the oil from the oil/water interface due to the hydrophobic properties possessed by the composite. The fabricated foam also possesses unique characteristics such as ultralightweight, high porosity, and recyclability. Attractive properties possessed by mCNT-MFC for such applications open new prospects for potentially sustainable water remediation applications.

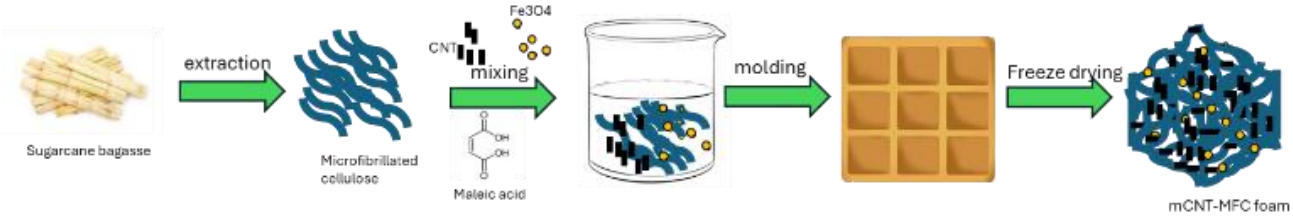

Figure 1. Diagram for the synthesis of mCNT-MFC composite foam

2.0 METHODS AND MATERIAL

2.1 Materials

Sugarcane bagasse (SCB), sodium hydroxide (NaOH), hydrogen peroxide (H_2O_2), sulfuric acid (H_2SO_4), sodium chlorite ($NaClO_2$), acetic acid, maleic anhydride, sodium hypophosphite, magnetic iron oxide (Fe_3O_4) nanoparticles, carbon nanotubes (CNT), engine oil, hexane, red palm oil, rice bran oil, peanut oil, distilled water, and deionized water.

2.2 Extraction of Microfibrillated Cellulose from Sugarcane Bagasse

The sugarcane bagasses (SCB) were sun-dried and ground using a grinder until it reached 100 µm in size. The SCB powders (25 g) were mixed with 500 ml of 2% (w/v) of NaOH and water bath for 5 hours at 80 °C in a water bath. The treated SCB were filtered and then bleached with 500 ml of H_2O_2 in a 1:1 aqueous dilution at 75 °C. The samples were further treated with 12% (w/v) NaOH solution and incubated in a water bath at 80 °C for 15 minutes. In order to completely break down the chemical bond of hemicellulose and lignin of SCB, the SCB was treated two times using NaOH. The treated SCB samples were vacuum filtered and washed a few times to ensure no NaOH and H_2O_2 residues were in the cellulose fibers' suspension. The treated SCB samples were further treated with 1% v/v of H_2SO_4 at 80 °C. The extracted samples were cleaned with distilled water until they achieved a neutral pH value. The samples were further treated by dispersing them in 5 wt.% NaOH solution under vigorous stirring for 24 hours at 75 °C. They were then washed with deionized water and filtered before being immersed in a mixture solution containing 2 wt.% $NaClO_2$ and acetic acid under stirring at 70 °C for 3 hours. The samples were then washed with deionized water several times before being stored in the refrigerator at 4 °C until further use.

2.3 Preparation of Crosslinked Microfibrillated Cellulose Foams

A weighted amount of crosslinkers (maleic anhydride and sodium hypophosphite) was added to the microfibrillated cellulose (MFC) suspension (0.6–2%) in water under mechanical stirring and finally treated in an ultrasonic bath for 10 minutes to obtain the native MFC aqueous solution. The aqueous solution was filled in a silicone cube mold and slowly chilled at a designated temperature (-80 ℃). The frozen samples will be dried for 4 days in a freeze-dryer at a condenser temperature of -84.5 °C.

2.4 Fabrication of Magnetic CNT-Microfibrillated Cellulose Foam

Magnetic CNT-microfibrillated cellulose (mCNT-MFC) foams were prepared by mixing magnetic iron oxide (Fe_3O_4) nanoparticles and CNT together with the MFC. Commercial Fe_3O_4 nanoparticles were used in this step. The weight ratio

of Fe_3O_4 in the Fe_3O_4/CNT nanocomposite slurry was kept constant throughout all of the samples. The slurry of Fe_3O_4/CNT nanocomposites in water was prepared by adding a weighted amount of MFC. The samples were then mixed in a water bath sonicator according to the designated time to obtain a homogenized mixture. The composite samples were stored at -20 ℃ overnight before being freeze-dried at different freezing temperatures for 4 days.

2.5 Optimization of mCNT-MFC Foams Preparation to Achieve the Highest Oil Loading

To study the response toward oil adsorption capacity, three (3) parameters (which include percentage of CNT, sonication time, and freezing temperature) for the preparation of mCNT-MFCs were selected and varied. The oil adsorption capacity was selected as the response for this study. The optimization study used Design Expert software version 6.0.0 (Stat-Ease Inc., Minneapolis, USA). Response surface method (RSM) and a three-level, three-factor factorial design were used to establish the experimental model. Table 1 shows the range of values selected for the optimization study. Optimization studies were conducted in triplicate (n = 3).

Table 1. Variable inputs for the optimization study

Parameters	Coded levels		
	-1	**0**	**1**
Percentage of CNT (%)	0.25	0.5	0.75
Freezing temperature (°C)	-140	-80	-20
Sonication time (min)	20	40	60

2.6 Oil Sorption and Reusability of mCNT-MFC Foams

The oil sorption experiment was carried out at room temperature. Five (5) ml of engine oil was added to a beaker. A piece of the foam sample was introduced into the beaker containing oil. After 5 minutes, the foam was collected and left to drain for 5 minutes to remove any excess oil. The mass sorption capacity (C) was calculated using the following equation:

$$C = \frac{(W_2 - W_1)}{W_1} \quad (1)$$

where W_1 and W_2 represent the weight of the foam before and after the oil sorption, respectively.

The sample with the highest oil sorption capacity based on the optimization study was further used to study the reusability of the sample. Absorbed oil was discarded by washing the sample with hexane, and the same procedure was repeated to demonstrate the reusability cycle of the foam. Oil sorption experiments and calculations of mass absorption capacity were carried out in triplicate (n = 3).

2.7 Sample Characterizations of mCNT-MFC Foam

Field emission scanning electron microscopy (FESEM) analysis was performed on the mCNT-MFC to investigate the microstructure of the samples, and the elemental analysis was confirmed via energy dispersive spectroscopy (EDS). The crystal structure and the composition of the mCNT-MFC composite were observed on X-ray Diffraction Analysis (XRD). Contact angle measurements were taken on a video contact angle to measure the surface wettability of the samples. The chemical functionality of the samples was measured by Fourier transform infrared (FTIR) spectra and was recorded in the transmittance mode in the range of 4000–400 cm^{-1} with a resolution of 4 cm^{-1}. Thermal stability measurements of the foams were carried out using a thermal analyzer at a heating rate of 10 °C/min under a nitrogen atmosphere (flow rate about 100 ml/min) from 25 °C to 600 °C. All characterization analyses were repeated three times (n = 3), and average values were reported.

2.8 Kinetics of Oil Sorption

The mCNT-MFC foam was prepared using optimized parameters suggested by the model. The kinetic oil sorption study was performed using four (4) different types of oil: engine oil, red palm oil, rice bran oil, and peanut oil. The amount of absorbed oil with time was recorded and calculated using Eq. (1). Kinetic studies were performed in triplicate (n = 3).

3.0 RESULTS AND DISCUSSION

3.1 Physicochemical Properties of mCNT-MFC

The synthesis procedures are summarized in Figure 1. Figure 2 shows the digital images of mCNT-MFC foam development, starting from dried and cleaned sugarcane bagasse in Figure 2(a) to ground bagasse in Figure 2(b). Figure 2(c), on the other hand, shows the crosslinked MFC foam. Treated microfibrillated celluloses were extracted from ground bagasse and mixed with a binder, followed by the freeze-drying step. Figure 2(d), on the other hand, shows the image of the mCNT-MFC foam, which is the final product. The dimensions of the mCNT-MFC foam samples were kept constant at 1.5 cm x 1.5 cm x 1.5 cm, and the mass and density were measured at 0.50 g and 0.15 g/cm^3, respectively. In comparison

to dense bulk materials, foam structure combines the advantages of having a light structure, an increased surface-to-weight ratio, and being permeable for fluid adsorption.

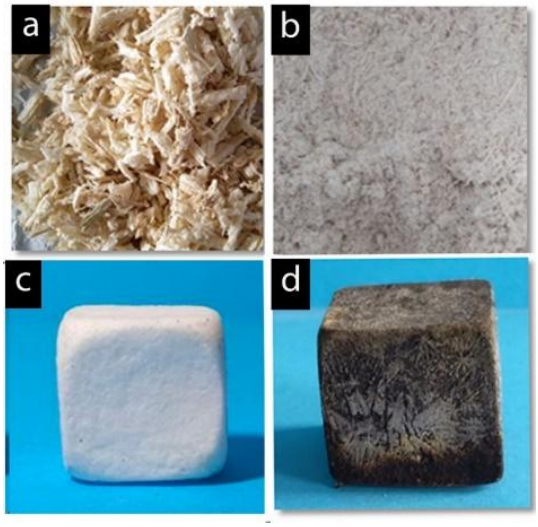

Figure 2. Digital images of (a) cleaned and dried sugarcane bagasse, (b) ground sugarcane bagasse, (c) MFC foam, and (d) mCNT-MFC foam

3.2 Optimization of the Oil Sorption Capacity

The RSM design optimized three (3) significant factors: the percentage of CNT (%), freezing temperature (°C), and sonication time (min) for the preparation of the mCNT-MFC foam. A total of 15 experimental runs were conducted, and the results are presented in Table 2. The percentage of CNT (%) was set from 0.25 to 0.75 (%), with a centre point of 0.5%. The freezing temperature ranged from -20 to -140 °C, with a centre point of -80 °C, while the sonication time varied from 20 to 60 min, with a centre point of 40 min, to assess their influence on oil sorption performance. An average of three replicates on oil sorption measurement was collected and presented in Table 2, and the data inserted for the oil sorption optimization was the average value of triplicate samples (n = 3) with an average standard deviation of 0.5.

The highest oil sorption of 5.05 g/g was achieved for samples 6 and 9, with a 0.75% CNT, -140 °C freezing time, and 20 minutes sonication time. In contrast, sample 4 yielded the lowest oil sorption capacity of 3.80 g/g. This sample was prepared with 0.25% CNT, a freezing time of -20 °C, and a 20-minute sonication time. The results suggested that higher CNT and higher freezing temperature lead to higher oil sorption capacity due to increased material hydrophobicity [11,12] and the possibility of closely and randomly packed microfibrillated fibre in the mCNT-MFC [9], respectively. Analysis of variance (ANOVA) for the oil sorption, as shown in Table 3, revealed that the model is significant with a p-value of 0.0006. A p-value of less than 0.05 implies that the model is significant. Similarly, the three selected parameters, which are the amount of CNT, freezing temperature, and sonication time, were also significant for the preparation of the sample with a p-value of 0.0027, 0.0025, and 0.0416, respectively. Similarly, the model F-value of 12.94 implies that the terms in the model have a significant effect on the responses. The optimal conditions for preparing the mCNT-MFC were suggested to be 0.73% CNT, a freezing temperature of -130 °C, and a sonication time of 20 minutes. These preparation parameters were used to prepare the sample for the recyclability and kinetic study.

Table 2. Engine oil sorption capacity based on Response Surface Method (RSM)

Run	Percentage of CNT (%)	Freezing temperature (°C)	Sonication time (min)	Engine oil sorption (g/g)
1	0.75	-20	60	4.27
2	0.25	-20	20	3.84
3	0.75	-20	60	4.32
4	0.25	-20	20	3.80
5	0.75	-140	20	4.73
6	0.75	-140	20	5.00
7	0.25	-140	60	4.13
8	0.5	-80	40	4.77
9	0.75	-140	20	5.05
10	0.5	-80	40	4.01
11	0.75	-20	60	4.21
12	0.5	-80	40	4.70
13	0.25	-140	60	4.59
14	0.25	-140	60	4.59
15	0.25	-20	20	4.22

Table 3. Analysis of variance results for oil sorption capacity

Source	Sum of Squares	df	Mean Square	F-value	p-value	
Model	1.70	3	0.5656	12.94	0.0006	significant
A-Percentage of CNT	0.6466	1	0.6466	14.80	0.0027	
B-Freezing temperature	0.6593	1	0.6593	15.09	0.0025	
C-Sonication time	0.2322	1	0.2322	5.31	0.0416	
Residual	0.4807	11	0.0437			
Lack of Fit	0.1120	6	0.0187	0.2530	0.9378	not significant
Pure Error	0.3688	5	0.0738			

3.3 Microstructure of mCNT-MFC Composite Foam

The morphologies of the mCNT-MFC sample in Run 9 are presented in Figure 3. From Figure 3(a), the interconnected structure of the cellulose microfiber (diameter of <10 μm) with porous areas is observed. At a higher magnification of 50k, the CNT network is observed throughout the body string of cellulose microfiber with no obvious aggregation of the nanoparticles (Figure 3(b)). Figure 3(c) shows a close-up sample image to further confirm the presence of CNTs with an average diameter of around 20 nm. Figure 2(d), on the other hand, shows the presence of Fe_3O_4 nanoparticles with a diameter of around 600-800 nm (yellow box) on the cellulose microfiber surface with possible aggregation of CNTs on the MFC framework. EDS data presented in Figure 3(e) confirms the presence of cellulose, CNT, and Fe_3O_4 in the 3D framework, where the intense peak of carbon compound representing CNT and cellulose is 49.6%, oxygen (O) from cellulose and Fe_3O_4 is 24.3% while iron (Fe), presenting the Fe_3O_4, is 14.8 wt.%. A small percentage of Na and Cl were also detected, which could be the residues during the extraction of the microfibrillated cellulose, or the binder used to prepare the composite material.

3.4 Physical and Chemical Properties of mCNT-MFC Composite Foam

To further confirm the composite structure of mCNT-MFC foam, X-ray diffraction (XRD) patterns (Figure 4(a)) and FTIR spectra (Figure 4(b)) of the mCNT-MFC foams were collected, analyzed, and compared with MFC alone and MFC with CNT (CNT-MFC). The MFC alone (purple colour spectra) shows characteristic peaks located at 14.0, 16.5, and 20°, 22.3° corresponding to the $(1\bar{1}0)$, (110), (200), and (200) diffraction planes, respectively, which are typical XRD patterns of cellulose II presenting a stable crystalline form. CNT-MFC (orange colour spectra) on the other hand shows the additional characteristic peak at 19.9°, 22.7°, 26°, 27.9°, 30°, and 33° corresponding to diffraction planes of (100), (101), (002), (111), (200), and (004) lattice plane of hexagonal graphite structure which confirmed that CNT successful incorporation of CNTs into the MFC framework. Meanwhile, the mCNT-MFC (black colour spectra) foam exhibits major crystalline phases belonging to metallic Fe, which is attributed to Fe_3O_4, besides those characteristics of cellulose and CNT. The characteristic peaks of Fe_3O_4 were located at 22.8°, 28.5°, 29.7°, 30.34°, 35.79°,43:26°, 53:84°, 56:81°, and 63.01° corresponding to the reflections from the (100), (004), (101), (220), (311), (400), (422), (511), and (440).

FTIR spectra for MFC show that the absorption band at 3391 cm^{-1} is assigned to hydroxyl groups stretching. Bands at 2906 cm^{-1} and 1373 cm^{-1} are assigned to stretching and deformation vibrations of the C–H group in the glucose unit. The new addition of a weak C–C bending peak around 500–700 cm^{-1} an absorption peak at 2924 cm^{-1}, which is attributed to symmetric and asymmetric CH_2 stretching and two intense peaks observed between 580 cm^{-1} and 630 cm^{-1}, which are attributed to the stretching vibration mode associated with the metal-oxygen Fe-O bonds in the crystalline lattice of Fe_3O_4, were observed on the mCNT-MFC foams presenting the CNT and Fe_3O_4, respectively. These observations confirmed that the composite was bound through physical interaction without involving chemical changes. Contact angle measurement, as shown in Figure 4(c), shows that the cellulose sample has a contact angle of less than 90° for MFC alone and 101° for MFC embedded with CNT nanoparticles (mCNT-MFC). This shows that the mCNT-MFC sample possesses hydrophobic properties, which are an important requirement for oil-sorbent materials apart from porous structures.

According to the thermogravimetric analysis (TGA) shown in Figure 4(d), the initial weight loss for the untreated MFC (red line) begins around 50 °C, likely due to the evaporation of moisture. By 100 °C, the sample experiences a large weight loss of approximately 15%. The decomposition becomes more pronounced with increasing temperature, to about 80% weight loss at 600 °C. The result indicates structural components and organic residues that degrade under this temperature range [13]. Due to this behaviour, the untreated MFC foam will dissolve easily in water, eventually disrupting the foam structure. This trend is also observed in the MFC (black line) sample, and it appears to have more thermal stability, where it experiences about 12% weight loss by 100 °C, with just over 55% total weight loss at 600 °C. It appears that improved matrix stability was achieved in the presence of maleic acid as a crosslinker agent, as indicated by the reduced weight loss compared to untreated MFC. Compared to MFC alone, CNT-MFC (green line) and mCNT-MFC (blue line) show better thermal resistance with an initial weight loss of less than 10% observed at 100 °C due to a moisture loss. The weight loss progresses slowly, with approximately less than 45% loss at 600 °C. The reduced weight loss in CNT-MFC and mCNT-MFC can be attributed to the effective dispersion and strong interaction between the CNTs and the MFC matrix, which restricts the decomposition of the organic components and enhances the overall thermal performance of the composite [14][15].

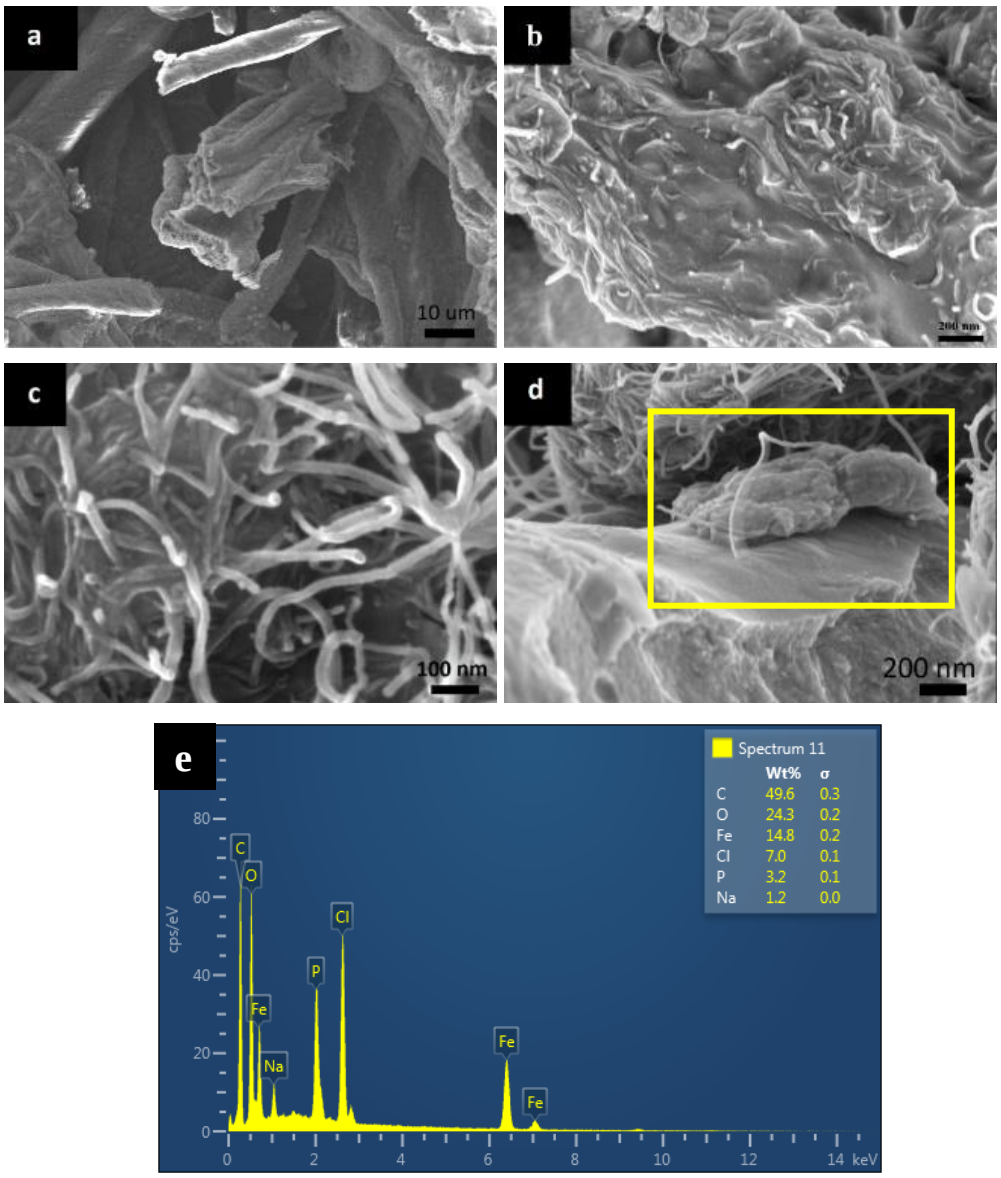

Figure 3. Morphology of mCNT-MFC observed using FESEM at (a) 1k, (b) 50k, (c) 80k, and (d) 100k magnification. The red box in (d) represents the Fe_3O_4 nanoparticles, and (e) energy-dispersive X-ray spectroscopy (EDS) spectrum of the mCNT-MFC nanocomposite foam

3.5 Recyclability Test of mCNT-MFC

Figure 5 shows the recycling experimental result of mCNT-MFC as an oil sorbent material. In this test, engine oil was used, and the sorption capacity was assessed in three separate trials using the same sample. After each trial, the oil was desorbed by soaking the sample in a hexane solution for several minutes, followed by oven drying before using it for the subsequent cycle. It was found that the oil sorption capacity was reduced by 50% in the second cycle and further reduced to 75% in the third cycle compared to that obtained for the first cycle. The results suggest that the mCNT-MFC can be reused for subsequent oil sorption, but with reduced oil sorption performance over time. This reduction of oil sorption capacity could be due to two (2) possible reasons: 1) incomplete removal of the oil from the previous cycle by the current hexane dissolution method, and ii) reduction of sample hydrophobicity due to the possibility of CNT leaching. Despite the reduction of oil sorption capacity, the CNT-MFC sample remains intact in its 3D foam structure, which suggests the recyclability potential of the sample. Compared to other cellulose-based oil sorbent materials [16][17], which can retain over 80% of their capacity after multiple cycles, our study offers a new cellulose-based oil sorbent material that is reusable due to its mechanically and thermally stable structure, as supported by the data provided in Figure 4. The recyclability performance of mCNT-MFC is comparable or slightly lower but remains promising given its eco-friendly origin from agricultural waste (e.g., a chitosan–cellulose aerogel retained over 85 % of its initial capacity after 50 sorption–desorption cycles) [22].

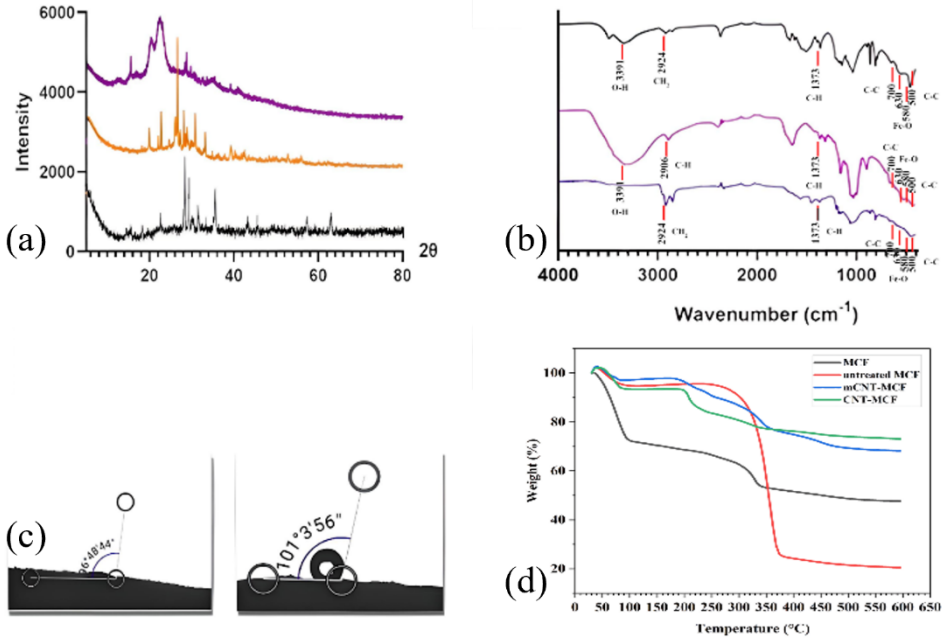

Figure 4. (a) XRD pattern, (b) FTIR spectra, (c) contact angle, and (d) TGA analysis of the CNT-MFC composite foam

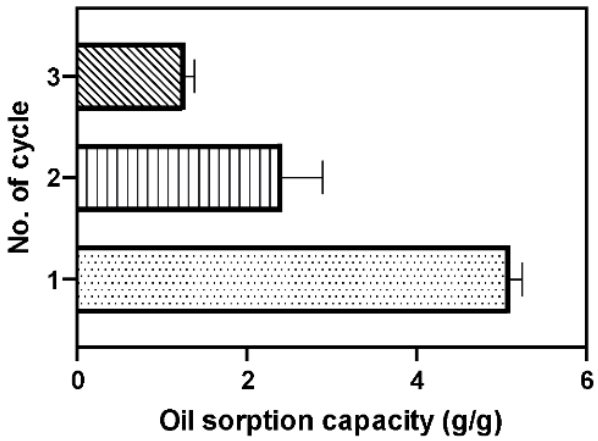

Figure 5. Recyclability of the mCNT-MFC composite foam by dissolution in hexane after oil sorption

3.6 Oil Absorption Capacity Test

The optimized mCNT-MFC was further assessed using different types of oil to see its sorption capacity. Three (3) other vegetable oils, namely red palm oil (RPO), rice bran oil (RBO), and peanut oil (PO), were evaluated for oil sorption using the mCNT-MFC foam for a shorter period, which is 90 sec. It was observed that almost similar amounts of oil were adsorbed by the mCNT-MFC, which are ~1 g/g for engine oil, RBO, and PO. This data shows that the mCNT-MFC has versatile performance towards different types of oil. Meanwhile, slightly less oil sorption was obtained for RPO might be due to the characteristics of RPO, which has a higher viscosity and forms a semi-solid at room temperature, primarily due to its higher saturated fat content [18][19]. Figure 6 supports the data in Table 4, which demonstrates efficient oil sorption (RPO, RBO, and PO) by the mCNT-MFC even at brief periods of time. Slightly more RPO remains in the beaker after adsorption than RBP and PO. It is also demonstrated that the mCNT-MFC foam remains intact during and after oil sorption with no visible sample leachate in the oil. The stable structure of the microfibrillated cellulose network was due to the presence of a linker that holds the microfibrillated cellulose networks. It has been reported that using a combination of maleic acid and sodium hypophosphite as a durable press finishing agent offers a safer yet equally effective alternative to traditional formaldehyde-based cross-linking agents for finishing cellulose-based fibres [20]. When compared with recent biosorbents reported in literature, the oil sorption capacity of mCNT-MFC (~1 g/g for various oils) falls within a slightly lower to comparable range, e.g., a chitosan/cellulose aerogel showed 13.8–28.2 g/g capacity, reusable for at least 50 cycles but the structural integrity and recyclability of mCNT-MFC highlight its practical advantages [23].

Table 4. Kinetics of oil sorption by mCNT-MFC composite foam

Type Oil	Density (g/cm^3) (at ~ 25 °C)	Weight before oil	Oil Absorption Capacity (g/g)
		0 s	90 s
Engine Oil	0.84 – 0.91	0.80	1.15
Red Palm Oil (RPO)	0.90 – 0.93	0.75	0.67
Rice Bran Oil (RBO)	0.913 – 0.920	0.72	1.00
Peanut Oil (PO)	0.912 – 0.920	0.81	0.94

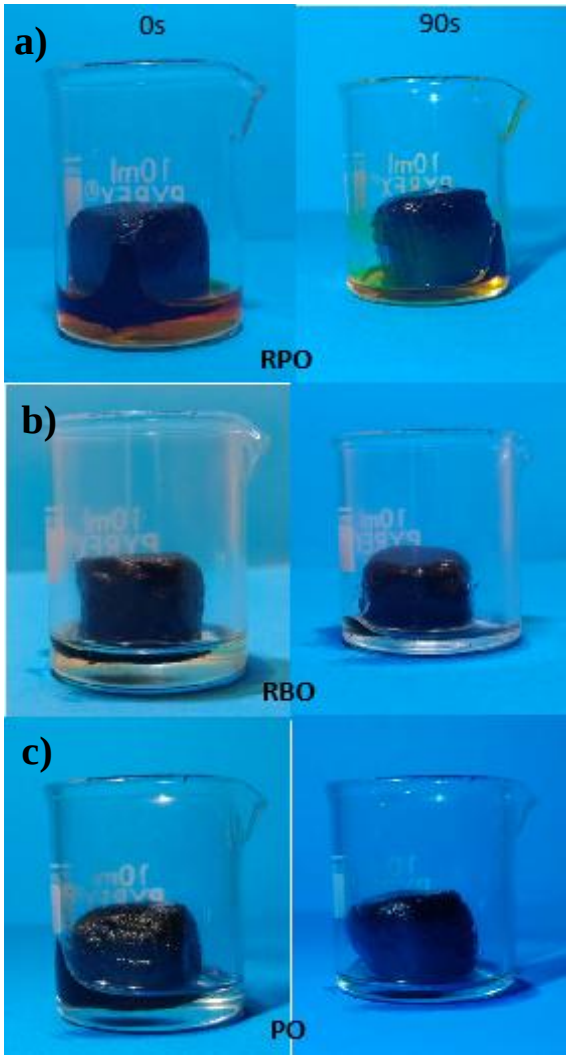

Figure 6. Oil sorption experiment with different types of oil before and after absorption of oil: a) Red palm oil, b) Rice bran oil, and c) Peanut oil

The oil sorption capacity of the mCNT-MFC composite foam over time, as depicted in Figure 7, shows slightly distinctive absorption behaviours for four (4) different oils. Engine oil demonstrated the fastest absorption, starting at 0.80 g/g and rising to 1.04 g/g by 90 seconds, with an adsorption rate of 0.014 s^{-1}, indicating a high affinity for this low-viscosity oil. RPO, on the other hand, showed the slowest absorption, starting at 0.75 g/g and reaching only 0.67 g/g by 90 seconds, with an absorption rate of 0.007 s^{-1}. This slower rate likely results from its higher viscosity, which restricts penetration into the foam [19][21]. RBO and PO exhibited a moderate absorption capacity, both with an adsorption rate of 0.011 s^{-1}, reflecting a balance between absorption rate and oil flow within the foam. These results highlight the foam's suitability for rapid absorption of low-viscosity oils, which is advantageous for quick cleanup in spill scenarios.

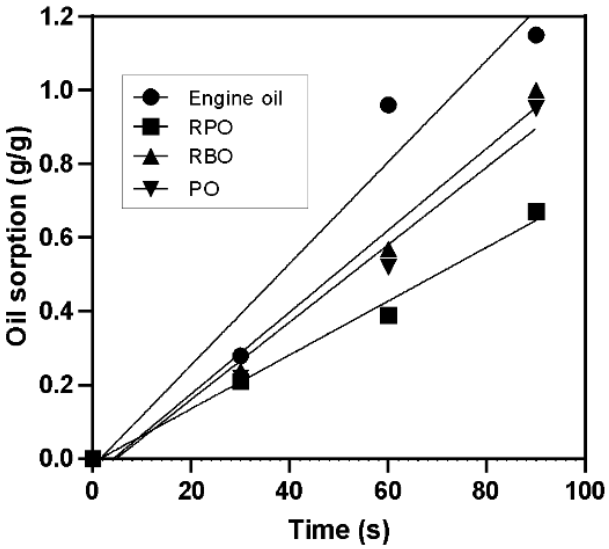

Figure 7. Oil sorption capacity with time for different types of oils

4.0 CONCLUSION

In summary, 3D microfibrillated cellulose foam derived from sugarcane bagasse cellulose embedded with CNT and magnetic particles as an oil sorbent material has been successfully developed. The mCNT-MFC composite foam consists of a porous network of microfibrillated cellulose and exhibits ultralightweight, hydrophobicity, and high selectivity towards oil. The mCNT-MFC composite foam has an adsorption capacity of 5.05 g/g, which is achieved when the samples are prepared using 0.75% CNT, -140 °C freezing temperature, and 20 minutes sonication time. The mCNT-MFC is a versatile oil sorbent material that can absorb engine and vegetable oil. Moreover, the sample can be recycled due to its intact structure with proper removal of the absorbed oil prior to the next oil sorption process.

Despite these promising results, some limitations remain. The present study was carried out in laboratory conditions with freshwater, and therefore, further testing in saltwater systems is necessary to assess performance in realistic marine spill scenarios. Additionally, large-scale synthesis, process economics, and long-term stability under repeated use require further investigation before industrial deployment can be realized. Future work should also focus on optimization of the foam structure for higher sorption capacity, evaluation of its biodegradability in natural environments, and cost-benefit analysis compared with existing commercial sorbents. Nevertheless, the current study presents a promising opportunity to use agricultural waste materials to help reduce oil spill incidents, which could yield substantial environmental advantages.

5.0 CONFLICT OF INTEREST

The authors declare no conflicts of interest.

6.0 AUTHORS CONTRIBUTION

Syazana Ab Manaf (Conceptualisation; Methodology; Validation; Formal analysis; Data curation; Visualisation; Writing - original draft)

Norsyamira Liyana Sulaiman (Conceptualisation; Formal analysis; Data curation; Formal analysis; Writing - review & editing)

Yusilawati Ahmad Nor (Conceptualisation; Methodology; Validation; Formal analysis; Data curation; Resources; Software; Visualisation; Writing - review & editing; Funding acquisition; Project administration; Supervision)

Dzun Noraini Jimat (Writing - review & editing; Resources; Supervision)

Kim Yeow Tshai (Writing - review & editing; Resources; Supervision)

7.0 ACKNOWLEDGEMENTS

The authors would like to express their gratitude for the financial support provided through the internal university (International Islamic University Malaysia) grant (Grant No.: RC-RIGS20-003-0003).

8.0 REFERENCES

[1] S. Ben Hammouda, Z. Chen, C. An, and K. Lee, "Recent advances in developing cellulosic sorbent materials for oil spill cleanup: A state-of-the-art review," *J. Clean. Prod.*, vol. 311, p. 127630, 2021, doi: 10.1016/j.jclepro.2021.127630.

[2] Y. Seida and H. Tokuyama, "Hydrogel adsorbents for the removal of hazardous pollutants—Requirements and available functions as adsorbent," *Gels*, vol. 8, no. 4, p. 220, 2022, doi: 10.3390/gels8040220.

[3] R. T. Varghese, R. M. Cherian, T. Antony, A. Tharayil, H. Das, H. Kargarzadeh, C. J. Chirayil, and S. Thomas, "A review on the best bioadsorbent membrane-nanocellulose for effective removal of pollutants from aqueous solutions," *Carbohydr. Polym. Technol. Appl.*, vol. 3, p. 100209, 2022, doi: 10.1016/j.carpta.2022.100209.

[4] P. Ieamviteevanich, D. Palaporn, N. Chanlek, Y. Poo-Arporn, W. Mongkolthanaruk, S. J. Eichhorn, and S. Pinitsoontorn, "Carbon nanofiber aerogel/magnetic core–shell nanoparticle composites as recyclable oil sorbents," *ACS Appl. Nano Mater.*, vol. 3, no. 4, pp. 3939–3950, 2020, doi: 10.1021/acsanm.0c00818.

[5] S. Ibrahim, S. N. I. B. Baharuddin, B. Ariffin, M. A. K. M. Hanafiah, and N. Kantasamy, "Cogon grass for oil sorption: Characterization and sorption studies," *Key Eng. Mater.*, vol. 775, pp. 359–364, 2018, doi: 10.4028/www.scientific.net/KEM.775.359.

[6] M. Zamparas, D. Tzivras, V. Dracopoulos, and T. Ioannides, "Application of sorbents for oil spill cleanup focusing on natural-based modified materials: A review," *Molecules*, vol. 25, no. 19, p. 4522, 2020, doi: 10.3390/molecules25194522.

[7] T. Aziz, A. Farid, F. Haq, M. Kiran, A. Ullah, K. Zhang, C. Li, S. Ghazanfar, H. Sun, R. Ullah, A. Ali, M. Muzammal, M. Shah, N. Akhtar, S. Selim, N. Hagagy, M. Samy, and S. K. A. Jaouni, "A review on the modification of cellulose and its applications," *Polymers*, vol. 14, no. 15, p. 3206, 2022, doi: 10.3390/polym14153206.

[8] O. Laitinen, T. Suopajärvi, J. A. Sirviö, and H. Liimatainen, "Superabsorbent aerogels from cellulose nanofibril hydrogels," *Cellulose-Based Superabsorbent Hydrogels*, 2018, doi: 10.1007/978-3-319-76573-0_20-1.

[9] F. Rafieian, M. Hosseini, M. Jonoobi, and Q. Yu, "Development of hydrophobic nanocellulose-based aerogel via chemical vapor deposition for oil separation for water treatment," *Cellulose*, vol. 25, pp. 4695–4710, 2018, doi: 10.1007/s10570-018-1867-3.

[10] S. Ab Manaf, A. M. Afandi, Y. A. Nor, D. N. Jimat, and N. A. Jamal, "Carbon fiber aerogel from nanofibrillated cellulose of sugarcane bagasse and waste engine oil residue for oil sorption," *Chem. Nat. Resour. Eng. J.*, vol. 7, no. 2, pp. 54–65, 2023, doi: 10.31436/cnrejv7i2.97.

[11] L. Calabrese, E. Piperopoulos, V. S. Jovanovic, V. Mitic, M. Mitic, C. Milone, and E. Proverbio, "Oil spill remediation: Selectivity, sorption, and squeezing capacity of silicone composite foams filled with clinoptilolite," *J. Appl. Polym. Sci.*, vol. 139, no. 29, p. e52637, 2022, doi: 10.1002/app.52637.

[12] J. Yen Tan, S. Yan Low, Z. H. Ban, and P. Siwayanan, "A review on oil spill clean-up using bio-sorbent materials with special emphasis on utilization of kenaf core fibers," *BioResources*, vol. 16, no. 4, 2021.

[13] A. Mandal and D. Chakrabarty, "Studies on the mechanical, thermal, morphological, and barrier properties of nanocomposites based on poly (vinyl alcohol) and nanocellulose from sugarcane bagasse," *J. Ind. Eng. Chem.*, vol. 20, no. 2, pp. 462–473, 2014, doi: 10.1016/j.jiec.2013.05.003.

[14] N. Nurazzi, M. R. M. Asyraf, M. Rayung, M. N. F. Norrrahim, S. S. Shazleen, M. S. A. Rani, A. R. Shafi, H. A. Aisyah, M. H. M. Radzi, F. A. Sabaruddin, and R. A. Ilyas, "Thermogravimetric analysis properties of cellulosic natural fiber polymer composites: A review on influence of chemical treatments," *Polymers*, vol. 13, no. 16, p. 2710, 2021, doi: 10.3390/polym13162710.

[15] J. P. John, M. N. T. E., and B. S. T. K., "A comprehensive review on the environmental applications of graphene–carbon nanotube hybrids: recent progress, challenges and prospects," *Mater. Adv.*, vol. 2, no. 21, pp. 6816–6838, 2021, doi: 10.1039/D1MA00324K.

[16] M. A. Hubbe, O. J. Rojas, M. Fingas, and B. S. Gupta, "Cellulosic substrates for removal of pollutants from aqueous systems: A review. 3. Spilled oil and emulsified organic liquids," *BioResources*, vol. 8, no. 2, pp. 3038–3097, 2013, doi: 10.15376/biores.8.2.3038-3097.

[17] T. T. Nguyen, N. D. Loc, and T. V. Nam, "Modified methods of oil cleanup with cellulose–based adsorbents: A review," *Vietnam J. Biotechnol.*, vol. 14, pp. 96–120, 2023.

[18] C. H. Tan, C. J. Lee, S. N. Tan, D. T. S. Poon, C. Y. E. Chong, and L. P. Pui, "Red palm oil: A review on processing, health benefits and its application in food," *J. Oleo Sci.*, vol. 70, no. 9, pp. 1201–1210, 2021, doi: 10.5650/josess21108.

[19] Z. Gao, Y. Zhu, J. Jin, Q. Jin, and X. Wang, "Chemical–physical properties of red palm oils and their application in the manufacture of aerated emulsions with improved whipping capabilities," *Foods*, vol. 12, no. 21, p. 3933, 2023, doi: 10.3390/foods12213933.

[20] A. F. Lehrhofer, L. Fliri, M. Bacher, D. Budischowsky, I. Sulaeva, M. Hummel, T. Rosenau, and H. Hettegger, "A mechanistic study on the alleged cellulose cross-linking system: Maleic acid/sodium hypophosphite," *Carbohydr. Polym.*, vol. 346, p. 122653, 2024, doi: 10.1016/j.carbpol.2024.122653.

[21] R. Wahi, L. A. Chuah, T. S. Y. Choong, Z. Ngaini, and M. M. N. Nourouzi, "Oil removal from aqueous state by natural fibrous sorbent: An overview," *Sep. Purif. Technol.*, vol. 113, pp. 51–63, 2013, doi: 10.1016/j.seppur.2013.04.015.

[22] W. Wang, J.H. Lin, J. Guo, R. Sun, G. Han, F. Peng, S. Chi, and T. Dong, "Biomass chitosan-based tubular/sheet superhydrophobic aerogels enable efficient oil/water separation," *Gels*, vol. 9, no. 4, p. 346, 2023, doi:10.3390/gels9040346.

[23] Z. Li, L. Shao, W. Hu, T. Zheng, L. Lu, Y. Cao, and Y. Chen, "Excellent reusable chitosan/cellulose aerogel as an oil and organic solvent absorbent," *Carbohydrate Polymers*, vol. 191, pp. 183-190, 2018, doi: 10.1016/j.carbpol.2018.03.027.